Phonon sheets in superfluid ^{4}He: Dependence of sheet width on heater size

D. H. S. Smith and A. F. G. Wyatt
School of Physics, University of Exeter, Exeter EX4 4QL, United Kingdom
(Received 12 January 2009; revised manuscript received 10 March 2009; published 22 April 2009)

A short phonon pulse injected into liquid ^{4}He propagates away from the heater as a phonon sheet. The angular dependence of the energy flux has a mesa shape, i.e., a flat top, which is the phonon sheet, and steep sides. The mesa shape is caused by high energy phonon creation in the pulse along the symmetry axis; this depletes energy from the flux until the central portion of the pulse has a constant energy. The low energy phonons then occupy a thin sheetlike volume. We have measured the width of the phonon sheet from three heaters of different widths at different heater powers and distances from the heater. We find the remarkable result that the sheet width is inversely proportional to the width of the rectangular heater. Also the height of the mesa falls off as the inverse square of the distance from the heater. We present a phenomenological model for the phonon propagation in liquid helium at 0 bar, which predicts these dependencies. It also predicts that the sheet width is proportional to the heater pulse length, and is only a weak function of heater power, both of which are seen experimentally.

DOI: 10.1103/PhysRevB.79.144520 PACS number(s): 67.10.−j

I. INTRODUCTION

Among the spectrum of possibilities for phonon systems in liquid ^{4}He, there are two extreme systems that can be created. One system is a very strongly interacting set of phonons which propagates as a whole in an anisotropic equilibrium. The other is a very weakly interacting set of phonons which propagates ballistically without scattering.

The strongly interacting group comprises of a dense collection of low energy phonons, *l*-phonons, with a typical energy $\epsilon/k_B \sim 1$ K. We can imagine the *l*-phonons occupying a cone of states cut from an equilibrium isotropic distribution at temperature T_p. So the energy of the *l*-phonon system is the fraction $\Omega/4\pi$ of the energy density of an isotropic distribution at a temperature T_p, where Ω is the solid angle of the occupied cone in momentum space which is typically 0.1 sr. T_p varies from ~ 1 K near the heater to ~ 0.6 K at >10 mm from the heater.[1] This is the Bose-cone approximation of an anisotropic phonon system, see, for example, Ref. 1.

The weakly interacting group consists of high energy phonons, *h*-phonons, with typical energy $\epsilon/k_B \geq 10$ K and relatively very low number density.[2] The two groups are illustrated in Fig. 1 where we show the signal from a short heater pulse detected after 12.3 mm. The low energy phonons arrive first and create the sharp peak at 52 μs, and the high energy phonons first arrive at the same time and peak at 65 μs.

The two phonon systems arise from the fact that low energy phonons can scatter by three phonon processes (3pp) (Refs. 3–5) but phonons with $\epsilon/k_B \geq 10$ K can only scatter by four phonon processes (4pp).[6–8] The 3pp scattering rate is very much higher than the 4pp scattering rate for the same number density of phonons.

The different scattering processes which are allowed depend on the phonon-dispersion curve. At the saturated vapor pressure, the dispersion is anomalous in the energy ranges $0 < \epsilon < \epsilon_c$ and $0 < q < q_c$, where ϵ and q are the energy and wave number of the phonon, respectively,[9,10] and $\epsilon_c = c\hbar q_c = 10 k_B$K, where c is the low-frequency velocity of sound, $c = 238$ ms^{-1}. As the dispersion curve rises above the normal linear dispersion at low q, i.e., $\epsilon(q) > c\hbar q$, then a low energy phonon can annihilate and create a pair of new phonons. The reverse process is also possible. Momentum is conserved by the pair of phonons having an angle between them so that $\mathbf{q}_1 = \mathbf{q}_2 + \mathbf{q}_3$ and $\epsilon_1 = \epsilon_2 + \epsilon_3$.

For $\epsilon/k_B \geq 10$ K, the phonon dispersion is normal, i.e., $\epsilon(q) < c\hbar q$, and three phonon processes are not allowed as momentum and energy cannot be conserved. Thus, at these energies, the fastest scattering is 4pp where two phonons combine to create two new phonons with $\mathbf{q}_1 + \mathbf{q}_2 = \mathbf{q}_3 + \mathbf{q}_4$ and $\epsilon_1 + \epsilon_2 = \epsilon_3 + \epsilon_4$. Here phonon 1 is the high energy phonon, i.e., $\epsilon_1 > \epsilon_c$, and the other three phonons can have more, or less, energy than ϵ_c.[4,8]

The spontaneous decay of a phonon by 3pp can occur for a lone phonon. If the *l*-phonons have a low number density, they will only spontaneously decay. The created phonons will continue to decay until the *l*-phonon number density is high enough for the reverse 3pp scattering to have a balancing rate. Under quite ordinary conditions of low initial number density, the reverse 3pp scattering rate can be negligible on the time scale of the experiment. This is because the 3pp scattering rate of phonon 1 in the process $\mathbf{q}_1 + \mathbf{q}_2 \rightarrow \mathbf{q}_3$ depends on the number density of phonon 2. However, phonon 2 must be at the right angle to interact with phonon 1, where the angle depends on the energies of phonons 1 and 2. Generally the angle must be small; it is usually much smaller than the maximum angle of 27° which is set by the extent of the anomalous dispersion. It is typically $\sim 10°$ so 3pp scattering is a small-angle scattering process.

For 4pp scattering, the scattering rate of phonon 1 depends on the number density of phonon 2, as well as on the energies ϵ_1 and ϵ_2, and wave vectors $\mathbf{q}_1$ and $\mathbf{q}_2$. The angle between the two wave vectors $\mathbf{q}_1$ and $\mathbf{q}_2$ must be large if phonon 1 is an *h*-phonon and phonon 2 is an *l*-phonon. If the angle is less than $\sim 50°$, energy and momentum cannot be conserved so the scattering rate is zero. As phonons are bosons, the scattering rate also depends on the occupation

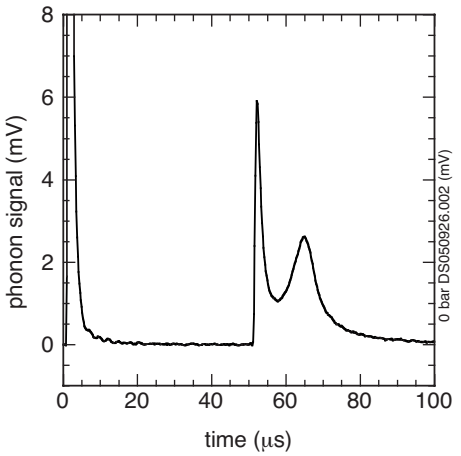

FIG. 1. Typical signals at $\theta=0$, using H1 and B1 (see Fig. 2). The first signal is from the *l*-phonons and the broader second signal is due to *h*-phonons. The heater pulse is 100 ns and 12.5 mW.

probability of the final states. This is usually a small effect as the final states have occupation probabilities $\ll 1$.

There are two usual situations when phonon 1 is an *h*-phonon. The first is when it is in a very low number density of other phonons. Then the *h*-phonon is not scattered and it just freely propagates ballistically. This occurs when an *h*-phonon is created in a short pulse of *l*-phonons propagating in cold liquid helium and is then left behind by the pulse because of its lower velocity. It is then alone in helium where there are few thermal excitations.

The second situation is an *h*-phonon created in a dense cloud of *l*-phonons. The *h*-phonons are concentrated along the propagation direction, as found experimentally[11] and theoretically.[12] Then, the *h*-phonon scatters with a *l*-phonon if there are *l*-phonons at a suitable angle. However, if the *l*-phonons are also confined to a narrow momentum cone along the propagation direction, as they are in a phonon pulse, then there are no *l*-phonons at a suitable angle, so again, the *h*-phonons are not scattered.

Besides the situations described above there is another very important 4pp scattering which occurs between two *l*-phonons, one of which has an energy fairly close to ϵ_c, say $8k_B$T and the other with say $3k_B$T. Then in the process $\mathbf{q}_1+\mathbf{q}_2\rightarrow\mathbf{q}_3+\mathbf{q}_4$, where $\mathbf{q}_1<\mathbf{q_c}$ and $\mathbf{q}_2<\mathbf{q_c}$, it is possible that $\mathbf{q}_3>\mathbf{q_c}$ and $\mathbf{q}_4<\mathbf{q_c}$. So, in this process an *h*-phonon $\mathbf{q}_3$ is created.[1,13] This can be a very efficient process. In a short pulse where the *h*-phonon is lost from the back of the pulse before it is scattered within the pulse (this defines a short pulse), then approximately half the initial energy in the *l*-phonon pulse, in the propagation direction, can be converted into *h*-phonons.

One of the interesting phenomena that occurs in a phonon pulse in cold superfluid helium, due to the 3pp and 4pp, is the formation of a mesa shaped angular phonon distribution. The top of the mesa constitutes a phonon sheet,[14] so called because it is a few millimeters wide and 24 μm thick, and has a uniform areal energy density. It is created by giving a short 10^{-7} s current pulse to a plane thin gold heater, typically 1×1 mm^2. A simplified picture is that a heating pulse of 100 ns duration creates a dense volume of *l*-phonons just in front of the heater, in a layer $ct_p=24$ μm thick. The phonons form a strongly interacting system of *l*-phonons which propagates away from the heater, along the heater normal, with a velocity which is indistinguishable from *c*.[15] The momentum distribution is mostly confined to a narrow cone whose axis is parallel to the heater normal.[11,12]

The mesa shape is formed because, as this *l*-phonon system propagates away from the heater, it creates *h*-phonons which reduce the energy density of the *l*-phonons to a constant value over a range of angles about the heater normal. This happens because the *h*-phonon creation rate depends strongly on the energy density in the *l*-phonon pulse. It drops to an insignificant rate when it reaches an energy density of $\mathcal{E}_h$. This energy density corresponds to the top of the mesa at the distance from the heater where this happens. A detailed theory of *h*-phonon creation and the energy loss from an *l*-phonon pulse as a function of distance has been given.[12] There may also be transverse expansion of the *l*-phonon system at large distances from the heater[16,17] which would assist in forming the mesa shape.

In this paper we experimentally investigate the effect of the size of the heater on the width of the mesa. We find a remarkable inverse relationship between the width of the mesa top and the heater width: a narrower heater creates a broader mesa. We present a simple phenomenological model which explains this effect and some other characteristics of the mesa.

In Sec. II we describe the experimental apparatus and method. In Sec. III, we present the measured angular distribution for three heater widths at different heater powers and distances, the signal at $\theta=0$ as a function of distance, and the mesa width for three heater widths. In Sec. IV we present our phenomenological model which explains the inverse relationship between heater width and the width of the mesa, and discuss the results. Conclusions are drawn in Sec. V.

II. EXPERIMENTAL METHOD AND APPARATUS

The experimental arrangement is shown in Fig. 2 and is the same as in Ref. 18. A substrate with three thin-film gold heaters is mounted on the axis of a holder with radial arms. The holder can be rotated by a stepping motor which drives through a worm gear. The angle θ of the rotor is measured by timing phonon pulses from the heaters mounted at the ends of the radial arms to fixed detectors which are $\sim$20 mm above them. In this way we obtain an angular accuracy of $\sim$0.3°. The main detector is mounted on the end of a vertical bar which is directly above the heater. This bar can move vertically and is driven by a second stepping motor through a cotton thread connection. The cross section of the bar is square, and the bar moves through a square sectioned guide channel so that its end is laterally positioned. The distance between the central 1×1 mm^2 heater and the bolometer is found from the time of flight of low energy phonons

Three thin-film gold heaters were evaporated onto a polished sapphire substrate 7.5 mm in diameter and 0.4 mm thick. The heater dimensions were 0.25×1, 1×1, and 0.5×1 mm^2. The rotation axis passed through the center of the 1×1 mm^2 heater. The long directions of the other two heat-

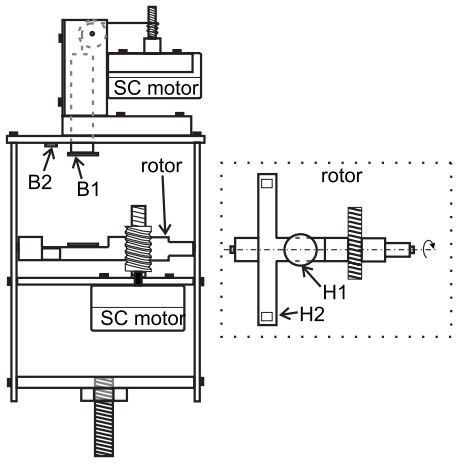

FIG. 2. Diagram of the apparatus. H1 is the central 1×1 mm^2 heater which is opposite the main bolometer B1. H2 and B2 are the heater and bolometer for the angular measurements. H1 and H2 are mounted on a rotor driven by a superconducting stepping motor. The separation of H1 and B1 is controlled by a second stepping motor.

ers were parallel to the rotation axis. As phonons propagate ballistically in sapphire, the opposite side of the sapphire disk was deliberately roughened so that it would diffusely reflect the phonons injected into the substrate and so distribute them over all angles. This means that very few of these phonons go into the liquid helium near the heater. In earlier experiments, with glass substrates there had been a low level but long tail to the detected phonon signal which came from phonons diffusing out of the glass substrate. With a sapphire substrate, there is a well defined single phonon pulse injected into the liquid helium and no thermal tail in the detected signal.

The detector was a zinc film evaporated on a polished sapphire substrate 10 mm in diameter and 1 mm thick. The zinc film was scratched into a serpentine track over an area of 1×1 mm^2. A superconducting solenoid gave a magnetic field that held the zinc near its superconducting transition boundary. The bolometer was in a bridge with electronic feedback that maintained it at a constant resistance and, hence, temperature of $\sim$0.35 K.[19–21] Recent experiments have shown that the sensitive area of the bolometer is actually only $\sim 0.1 \times 0.1$ mm^2.[22] It is most likely that the sensitive region is a single superconducting-normal boundary across the track width of $\sim$0.1 mm.

The apparatus was sealed in a brass cell that was filled with ultrapure liquid ^{4}He (Ref. 23) and could be pressurized up to 24 bar. The pressure was measured with a Budenberg standard test gauge to an accuracy of 0.02 bar. The cell was mounted on a dilution refrigerator which maintained the temperature of the cell at $\sim$50 mK during measurements.

The heater was pulsed by a Le Croy 9210 pulse generator with a repetition rate of 45 Hz. The signal was amplified with an EG and G 5113 preamplifier, and captured and averaged in a Tectronix DSA 601A to increase the signal-to-noise ratio.

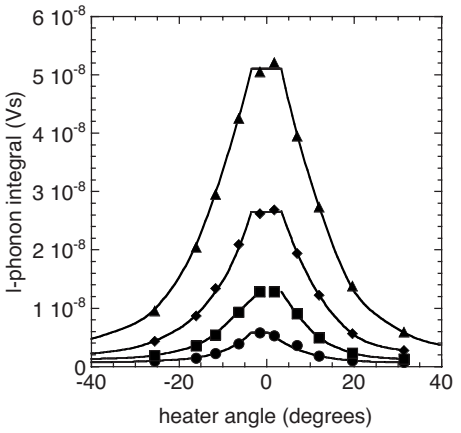

FIG. 3. The angular distribution of the signal for the 1×1 mm^2 heater, at the time of the *l*-phonon peak, at a heater-bolometer separation of 8.2 mm for heater powers of 3.125 (circles), 6.25 (squares), 12.5 (diamonds), and 25 mW (triangles). The heater pulse is 100 ns.

III. MEASURED ANGULAR VARIATION IN THE *L*-PHONON SIGNAL

The experimental procedure was to set the angle θ between the heater normal, and the line joining the heater and the bolometer, taking timing traces from which the angle can be determined and then measure the phonon signal at four different heater powers. Measurements with all the heaters were made at one heater-bolometer distance before moving to a new distance. From the signal as a function of time (see, for example, Fig. 1) the integral of the *l*-phonon peak is found by integrating the *l*-phonon signal numerically. The results are shown in Figs. 3 and 4 for the 1×1 mm^2 heater at 0 bar. In Fig. 4 we also show the angular distribution of

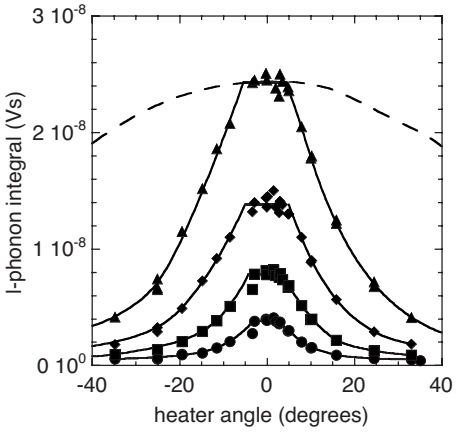

FIG. 4. The angular distribution of the signal for the 1×1 mm^2 heater, at the time of the *l*-phonon peak, at a heater-bolometer separation of 12.3 mm for heater powers of 3.125 (circles), 6.25 (squares), 12.5 (diamonds), and 25 mW (triangles). The heater pulse is 100 ns and the pressure is 0 bar. The dashed line is the angular distribution at 24 bar, 25 mW, and 12.3 mm, normalized to the height of the mesa, showing that there is no mesa at this pressure. At θ=0, the signal is 2.56$\times$ higher at 24 bar than at 0 bar (Ref. 18).

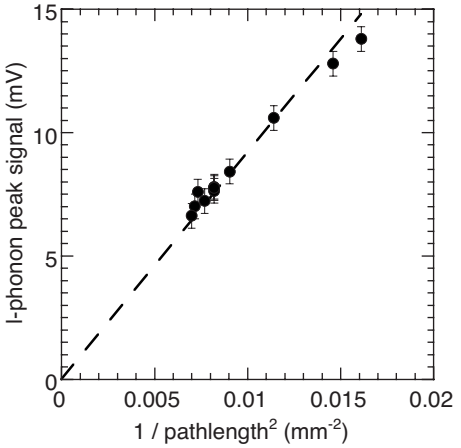

FIG. 5. The peak of the l-phonon signal is shown versus the inverse of the square of the distance between the 1×1 mm^2 heater and the bolometer B1. The angle $\theta=0$ and the heater pulse is 100 ns.

the l-phonon signal at 24 bar pressure, from Ref. 18. It can be clearly seen that there is no mesa shape at this pressure.

As the rotation axis passes through the center of the 1×1 mm^2 heater, the other two heaters do not rotate about an axis that passes through their centers. This means that the measured angular distribution for the off-axis heaters, instead of showing a horizontal mesa top, shows a straight line at an angle to the horizontal axis. The reason for this is that an off-axis heater is nearer the bolometer for say positive angles than for negative angles. To correct the measured angular distribution, we need to know how the signal changes with heater-bolometer distance. This was found by setting the heater angle to zero for the central heater, and then moving the bolometer toward this heater. The distance was calculated from the time of flight of the l-phonons and the velocity of sound, $c=238.3$ ms^{-1}. The results are shown in Fig. 5. We see to a good approximation that the l-phonon varies as the inverse square of the distance over this range of distances, where h-phonon creation is negligible.

This $1/R^2$ distance dependence immediately suggests that the shell of energy is expanding in a near ballistic way from a pointlike source. This is very interesting because the phonons at angles near zero are very strongly interacting and do not travel ballistically. We shall return to this point in Sec. IV.

We can now correct the measured signal as a function of angle. Consider a heater whose center is a distance a from the rotation axis, and this axis is a distance b from the bolometer. At a rotation angle θ, the heater-bolometer distance $R(\theta)$ is given by

$$R^2 = b^2 + a^2 + 2ab\ \sin\ \theta. \tag{1}$$

Hence the corrected signal $S(\theta)$ is related to the measured signal, $S_m(\theta)$, by

$$S(\theta) = \frac{S_m(\theta)}{1 + 2(a/b)\sin\ \theta + (a/b)^2}, \tag{2}$$

in practice $a/b \ll 1$.

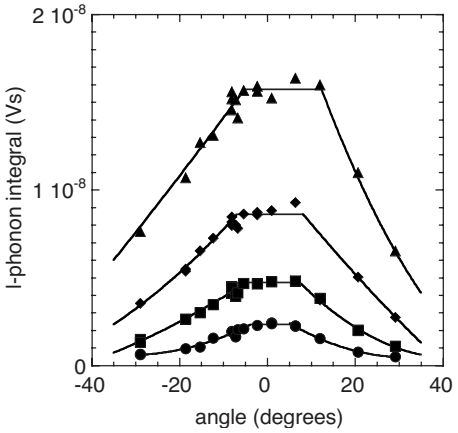

FIG. 6. The corrected angular distribution of the signal for the 0.5×1 mm^2 heater, at the time of the l-phonon peak, at a heater-bolometer separation of 12.3 mm for heater powers of 3.125 (circles), 6.25 (squares), 12.5 (diamonds), and 25 mW (triangles). The heater pulse is 100 ns.

Applying this to the data we get the results shown in Fig. 6 for the 0.5 mm heater at 12.3 mm, and Figs. 7 and 8 for the 0.25×1 mm^2 heater at 8.2 and at 12.3 mm, respectively, all at 0 bar.

We see that all the angular variations in Figs. 3, 4, and 6–8 have the same generic shape, as found in the previous measurement at 16.7 mm,[14] i.e., a flat top around $\theta=0$ and steeply falling sides. The present data do not show such a good flat mesa top as Ref. 14 but the present data are consistent with a flat top and we shall assume that it is so. The solid lines through the points in the angular dependencies are fitted with this assumption. The width of the mesa top is graphically defined by the intersection of the steep sides and the horizontal line of the mesa top.

The angular width of the mesas are shown in Fig. 9 as a function of power. Also shown is the data from Ref. 14. It is quite clear that the narrower the heater, the wider the mesa

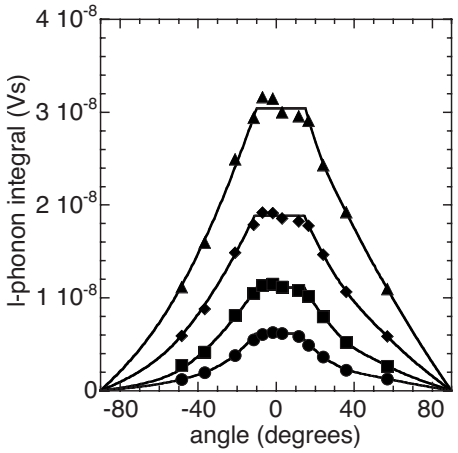

FIG. 7. The corrected angular distribution of the signal for the 0.25×1 mm^2 heater, at the time of the l-phonon peak, at a heater-bolometer separation of 8.2 mm for heater powers of 3.125 (circles), 6.25 (squares), 12.5 (diamonds), and 25 mW (triangles). The heater pulse is 100 ns.

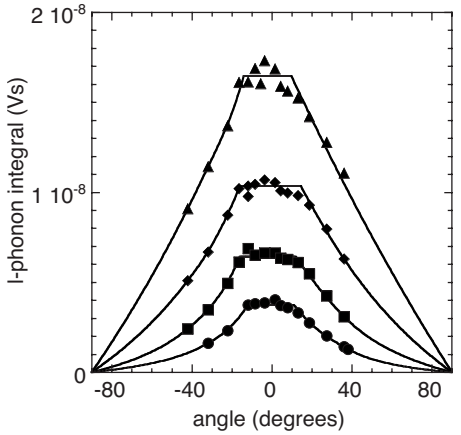

FIG. 8. The corrected angular distribution of the signal for the 0.25×1 mm^2 heater, at the time of the *l*-phonon peak, at a heater-bolometer separation of 12.3 mm for heater powers of 3.125 (circles), 6.25 (squares), 12.5 (diamonds), and 25 mW (triangles). The heater pulse is 100 ns.

top. There is no systematic difference within the uncertainty between the data at 8.2 and 12.3 mm for the 0.25 mm wide heater. However, for the 1 mm wide heater, the mesa width is systematically wider for the 12.3 mm data than for the 8.2 mm data. This is confirmed by the curves in Figs. 3 and 4 which show that the full widths at half height of the angular dependencies are systematically smaller at 8.2 mm than at 12.3 mm for the 1 mm heater, but for the 0.25 mm heater, they are the same at 8.2 and 12.3 mm, see Figs. 7 and 8.

In Fig. 10 we plot the width of the mesa top (i.e., the sheet width) against $1/h$ for the three heaters at 12.3 mm and at four heater powers. We see that the mesa width is well described, within the experimental uncertainties, as being inversely proportional to the heater width. Only one data point, 25 mW into the 0.25×1 mm^2 heater, does not follow this behavior. The generally weak dependence of the width on heater power is evident in this figure.

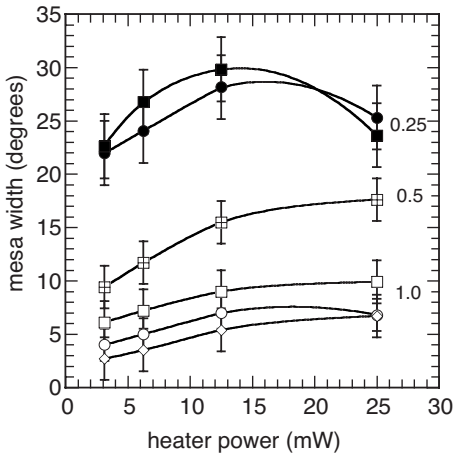

FIG. 9. The angular width of the mesa versus the heater power for the three heaters with widths of 1, 0.5, and 0.25 mm. The data for distance of 12.3 mm is shown by square symbols, and for 8.2 mm by round symbols. The data shown by diamonds symbols is for a 1 mm wide heater at 16.7 mm from Ref. 14. The heater pulse is 100 ns for all the data.

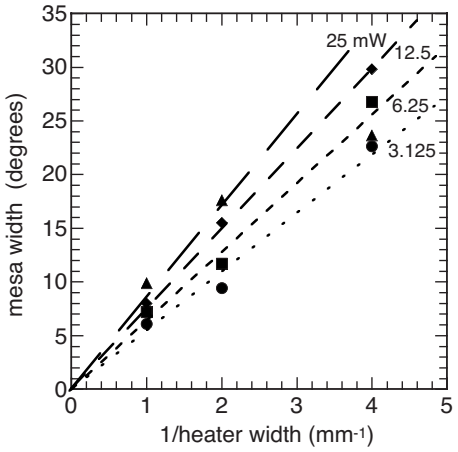

FIG. 10. The angular width of the mesa versus the inverse of the heater width for a heater-bolometer distance of 12.3 mm, for heater powers of 3.125, 6.25, 12.5, and 25 mW. The heater pulse is 100 ns.

In Fig. 11 we show the mesa height as a function of heater power for two heater-bolometer distances. We see that the areal energy density of the mesa increases with heater power in a slightly less than linear way. The signals from the widest heater, 1×1 mm^2, are much higher than those from the narrowest heater 0.25×1 mm^2. This indicates that the energy from the narrowest heater is more spread out in angle than it is from the wider heaters. We will return to this point when we discuss the model in the next section. The signals at 12.3 mm distance are about half those for the 8.2 mm distance for both the 1×1 and 0.25×1 mm^2 heaters. This is to be expected from the $1/R^2$ distance dependence as $(8.2/12.3)^2=0.44$.

IV. MODEL AND DISCUSSION OF RESULTS

We envisage that initially the pulse of phonons has an energy density which varies with angle from the symmetry axis; then, due to *h*-phonon creation, all parts of the pulse with $\mathcal{E}>\mathcal{E}_h$ will decrease in energy to $\mathcal{E}_h$. The parts of the pulse with $\mathcal{E}<\mathcal{E}_h$ initially will stay at the same energy density but the phonons, making up that density, will decrease in phonon energy and increase in number due to spontaneous 3pp decay and so give a smaller signal from the phonon-energy dependent detector. These processes gives the angular distribution a mesa shape, with the area of uniform density forming the mesa top and the phonons that have spontaneously decayed making up the sides of the mesa.

Although we wish to understand the formation of the mesa shape at 0 bar, we start by considering the superfluid helium at 24 bar because at this pressure the phonon propagation from the heater is ballistic. From this readily understandable situation we shall consider what happens when the pressure is reduced and phonons begin to interact.[24] Finally, at 0 bar we will have very strong interactions at small angles to the normal of the heater but only spontaneous phonon decay at large angles to the heater.

At 24 bar the energy from the heater has a cosinelike distribution at a distance which is an order-of-magnitude

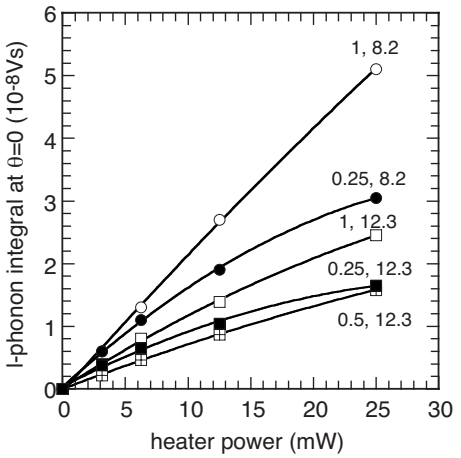

FIG. 11. The signal from the mesa top versus heater power for the three heater widths, the 1 and 0.25 mm heaters at 12.3 and 8.2 mm, and the 0.5 mm heater at 12.3 mm. The heater pulse is 100 ns.

larger than the heater width,[18] see dashed line of Fig. 4. The energy from a short heater pulse is contained in an almost spherical shell centered on the middle of the heater. The thickness of the shell varies with angle θ, heater width h, and radius of the shell R. If the heater were a point, then the thickness d of the shell would be just ct_p, where ct_p is the pulse length. However for a finite-size heater, the thickness $d=ct_p+h^2/8R$ at $\theta=0$. R is the distance from the center of the heater to the shell. Typical values are $ct_p=24$ μm and $h^2/8R=12.5$ μm for $h=1$ mm and $R=10$ mm. At larger angles the thickness of the shell rapidly increases due to the difference in the distance from each edge of the heater to a point on the shell, see Fig. 12. The thickness d, for $\theta > h/4R$, is given by

$$d = ct_p + h \sin \theta \tag{3}$$

to order $h^2/8R^2$, i.e., $\sim 10^{-3}$ for $h=1$ mm and $R=10$ mm. As θ increases, $h \sin \theta$ rapidly dominates ct_p. For example, at $\theta=10°$ and $h=1$ mm, $h \sin \theta=174$ μm which is much larger than $ct_p=24$ μm.

The energy in the low energy phonons is $\gamma W t_p$, where W is the heater power, t_p is the heater pulse duration, and γ is the fraction of the heater energy that goes into the low energy phonons. So $1-\gamma$ is the fraction of the energy that goes into the heater substrate at 24 bar. As the measured l-phonon energy at 24 bar varies with angle θ as $\cos \theta$,[18] so the energy per unit area of the shell, at angle θ and at distance R, is given by

$$E = \frac{\gamma W t_p \cos \theta}{\pi R^2}, \tag{4}$$

where the integrated energy over the half space is equal to $\gamma W t_p$.

Hence from Eqs. (3) and (4), the energy density $\mathcal{E}$ in the shell, for $R \gg h$, is given by

$$\mathcal{E} = \frac{E}{d} = \frac{\gamma W t_p \cos \theta}{\pi R^2 (ct_p + h \sin \theta)}. \tag{5}$$

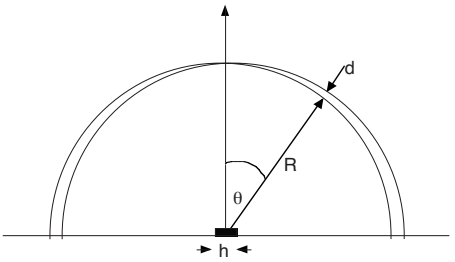

FIG. 12. A diagram of the geometry used in the model. The two semicircles enclosing the shell are centered on the two edges of the heater. The width of the heater is h and the thickness of the shell is d.

To obtain the energy density at 0 bar we assume that the angular distribution of the energy injected by the heater does not change much with pressure. In other words the transmission process across the interface between the heater and the liquid helium is a weak function of pressure. This is discussed in Ref. 25. Once the energy is in the liquid ^{4}He there will be interactions at small values of θ which will perturb this energy distribution but we shall argue below that, at large angles where the phonons are not strongly interacting, the energy flux remains much as it is at 24 bar although the phonons spontaneously decay. This implies that the energy density, to a first approximation, is the same as described by Eq. (5) in those regions where the phonons are weakly interacting. When the phonons are strongly interacting, the energy distribution will be modified due to h-phonon creation which depletes the energy in the shell. This process will give rise to the flat top of the mesa.

We divide the angular region into three at 0 bar, the small-angle region A, with $0 < \theta < \theta_A$, the intermediate region with $0_A < \theta < \theta_B$, and the large-angle region B, with $\theta_B < \theta < \pi/2$. At 0 bar, in angular region A the l-phonons are strongly interacting by 3pp scattering, which creates an anisotropic equilibrium. At distances within a few millimeters of the heater, these phonons have created h-phonons which have been lost to the pulse if it is a short pulse, which is what we are considering here. By about 5 mm from the heater, there is negligible h-phonon creation[26] and the l-phonons continue to propagate as an interacting system with a constant total energy. There may be some transverse expansion,[16,17] in which case θ_A will increase with distance from the heater, but we ignore any expansion in our model.

In the angular region B, there are noninteracting low energy phonons. These phonons do not interact with each other because their density is too low and this reduces the scattering rate which is inversely proportional to their number density. However these phonons do spontaneously decay so the average energy of these phonons considerably decreases with distance from the bolometer. Although the total energy in these phonons remains the same, our bolometer detector is less sensitive to phonons with lower energy[27] and this causes the signal to be much lower if the phonons spontaneously decay to lower energies.[24]

If phonons are not interacting and do not spontaneously decay, then they propagate ballistically. However if they spontaneously decay, the decay products are at an angle to

the initial phonon. This will lead to an angular broadening of the phonon flux about any initial direction. However the injected phonons have a relatively low energy, around $\epsilon/k_B \sim 2$ K and so the 3pp angles are small compared to the angular range of the B region. Under these conditions, the assumption that the phonons propagate along ballistic directions in the B region is a reasonably good approximation at $p=0$ bar. Nevertheless, the time integrated l-phonon signal at a given $\theta > \theta_B$ will be much smaller at 0 bar than at 24 bar for the reason given above.

The intermediate region between regions A and B certainly has a finite angular width. The phonon density is not negligible so there is some 3pp up scattering as well as phonon decay. The 3pp scattering is mostly to phonon energies well below $\epsilon_c/k_B=10$ K and so there is negligible 4pp scattering to phonons with $\epsilon/k_B > 10$ K, i.e., there is negligible h-phonon creation at any distance from the heater in the intermediate region. As the phonon density increases with decreasing angle, the 3pp up-scattering rate increases and so the average phonon energy is higher than in region B. Hence the detected signal increases. Again, because 3pp angles are small, the phonons travel in approximately ballistic directions in the intermediate region.

The angle θ_A, at the end of region A and the beginning of the intermediate region, is determined by the h-phonon creation rate just becoming negligible at angle θ_A and at a distance of several millimeters from the heater. The end of the intermediate region and the beginning of the B region is determined by the phonon number density being high enough for there to be a significant rate of 3pp up scattering at angle θ_B.

Close to the heater, the angular range of the three regions will depend on the distance from the heater. However, at distances beyond R_h, where phonon creation has dropped to a negligible rate, R_h is around 5 mm,[26] the angular ranges do not change much with distance. So the angular width of the mesa top is approximately constant for $R > R_h$ as is evident in Fig. 9.

The angular width of the mesa is equal to $2\theta_A$. We estimate the angular width, θ_A, of region A at $R=R_h$ in the following way. We calculate the phonon density in the intermediate region assuming that the phonon-energy flux is ballistic. As we have discussed, this is an approximation as there is small-angle 3pp scattering. Using Eq. (5) we find the energy density in the phonon shell at $R=R_h$. It is a strong function of angle due to the finite size of the heater. We then find the angle where the energy density is equal to the critical energy $\mathcal{E}_h$ density, where h-phonon creation becomes negligible.

This critical energy density corresponds to the l-phonon-energy density that is appropriately large enough to give a 3pp scattering rate which is appropriately high enough to create an equilibrium distribution, at a temperature and cone angle where h-phonon creation is negligible. $\mathcal{E}_h$ is appropriately the energy density, at R_h, of the mesa top at heater power W. Equating the energy density, given by Eq. (5), to the critical energy density at $R=R+h$, we get

$$\frac{\gamma' W t_p \cos\theta_A}{\pi R_h^2 (c t_p + h \sin\theta_A)} = \mathcal{E}_h, \tag{6}$$

where γ' is different from γ as it includes the fraction of the heater pulse energy that is lost from the l-phonons by h-phonon creation. From experiments we know that usually θ_A is large enough that $ct_p \ll h \sin\theta_A$.

We now consider why the critical energy density $\mathcal{E}_h$ depends on the heater power W. The scattering rate of a l-phonon with $\mathbf{q}_1$ is proportional to the number density of phonons with which it can scatter by 3pp, i.e., those phonons in a cone in momentum space with a cone angle θ_3. If the l-phonon system has an occupied cone in momentum space, with a cone angle θ_c, then only the fraction Ω_3/Ω_c of the l-phonons interact with phonon $\mathbf{q}_1$, where $\Omega_i = 2\pi(1-\cos\theta_i)$ is the solid angle associated with the cone angle θ_i. The minimum-energy density $\mathcal{E}_{\min}$ for h-phonon creation is when $\theta_c=\theta_3$, as in anisotropic system in equilibrium, θ_c cannot be smaller than θ_3. $\mathcal{E}_{\min}$ is a constant which is independent of heater power. The corresponding total-energy density is then $\mathcal{E}_h=\mathcal{E}_{\min}\Omega_c/\Omega_3$.

As the l-phonon pulse propagates, its cone angle increases due to it losing energy by creating h-phonons.[12] At a fixed distance of say 10 mm from the heater, the occupied solid angle in momentum space increases with the initial energy in the helium, i.e., with heater power. So as the heater power increases, a smaller fraction of the l-phonons interacts with any one phonon. Hence the critical energy density $\mathcal{E}_h$, for the critical scattering rate where h-phonon creation just becomes negligible, has to be higher at higher heater powers.

The bolometer signal is proportional to the energy in the whole of the occupied solid angle in momentum space,[14] and so the detected energy is proportional to the energy density in real space. As $\mathcal{E}_h=\mathcal{E}_{\min}\Omega_c/\Omega_3$, and $\mathcal{E}_{\min}$ and Ω_3 are constants, then as $\Omega_c \propto W$ so $\mathcal{E}_h \propto W$, all to zeroth order.

An expression for $\mathcal{E}_h(W)$ can only be found approximately. The general form for $\mathcal{E}_h(W)$ can be obtained from Eq. (5), putting $\theta=0$, $R=R_h$, and $\gamma=\gamma'$. Hence

$$\mathcal{E}_h(W) \approx \gamma' W/\pi R_h^2 c. \tag{7}$$

We now appeal to measured results. We note that $\mathcal{E}_h(W)$ corresponds to the height of the mesa top at distance R_h. At a distance $R > R_h$, the angular width of the mesa top is approximately constant and so the energy density $\mathcal{E}_{\text{mesa}}$ corresponding to the top of the mesa decreases as $1/R^2$, i.e., $\mathcal{E}_{\text{mesa}}=\mathcal{E}_h(R_h/R)^2$. In Fig. 11, where the l-phonon signal is plotted against the heater power W, we see that $\mathcal{E}_{\text{mesa}}$ increases slower linearly than with W. So we multiply W, in Eq. (7), by a factor f where $f=S/gW$, S is the height of the mesa top, and g is the ratio $g=S/W$ as $W \to 0$ in Fig. 11. So $f=1$ at low heater powers but decreases a little to below one as the heater power increases. The numerical coefficient needed to multiply the right side of Eq. (7) cannot be determined from an integral over the half space as can be done with Eq. (4). Hence we introduce a proportionality constant a. So we obtain

$$\mathcal{E}_h(W) = \alpha\gamma' f W/\pi R_h^2 c. \tag{8}$$

Using expression (8) in Eq. (6) and neglecting the term ct_p in the bracket, as it is found from measurements to be small compared to $h \sin \theta_A$, we finally have

$$\tan \theta_A = \frac{ct_p}{afh}. \quad (9)$$

The value of a from measured widths of the mesa is ≈ 0.4.

We see from Eq. (9) that $\tan \theta_A$ is proportional to $1/h$, t_p, and $1/f$. In Fig. 10 we see that the mesa width increases as the heater width decreases. At the three lowest heater powers the mesa widths show a $1/h$ dependence within the experimental uncertainties. At the highest power, the 1 and 0.5 mm heaters scale as $1/h$ but the mesa width for the 0.25 mm heater, at the highest power, falls well below this scaling. Perhaps it is due to the very high heater power density for this data point.

The dependence of θ_A on heater power is only through f which is a slowly decreasing function of W. From Fig. 10, we see that the gradients of the curves at different powers are fairly similar which shows that the mesa width is only weakly dependent on heater power. However as the heater power increases, f decreases and, from Eq. (9), the mesa width increases. This is the behavior of the gradients in Fig. 10.

In the present experiments we did not measure the pulse length dependence of the mesa width but it was measured previously.[14] There it was found that the mesa width doubled as t_p increased from 50 to 100 ns. This again is in agreement with Eq. (9). For $t_p > 100$ ns the mesa width did not increase linearly with t_p but this is to be expected as the heater pulse ceases to be a short pulse for $t_p > 100$ ns. In which case the h-phonons are not completely lost from the l-phonon pulse and so the process for creating the mesa is increasingly less effective. Hence for $t_p > \sim 100$ ns the mesa width only slowly increases with t_p, as was seen.

V. CONCLUSIONS

In this paper we have presented measurements of the angular dependence of the flux of low energy phonons from three different size heaters into liquid ^{4}He which is in such a low temperature that there are a negligible number of thermal excitations. The liquid helium is at 0 bar pressure so that the low energy phonons strongly interact by three phonon scattering when their density is sufficiently high.

Over the distance range of 8.2–12.3 mm we found that the signal varies as the inverse square of the distance R, see Fig. 5. This is the dependence one would expect from a point source from which the phonons propagate ballistically. However at angles close to the symmetry axis the phonons are interacting very strongly. Nevertheless the $1/R^2$ dependence strongly suggests that, at distances far from the heater, the energy is radiating out in a thin shell in a near ballistic way. We use this idea in the model to obtain Eq. (7).

The measured angular dependencies for the three heaters are shown in Figs. 3, 4, and 6–8, and they all show a mesa shape. The width of the mesa top is well defined by the height of the top and the steep slopes on each side. Their angular width varies as the inverse of the heater width. This striking result is shown in Fig. 10 at a distance of 12.3 mm. The mesa angular widths are weak functions of heater power and distance, see Figs. 9 and 10.

The height of the mesa measures the areal energy density of the phonon sheet. It increases with heater power but in a below linear way, as shown in Fig. 11. The widest heater shows the highest mesa which is to be expected as the widest heater keeps the energy concentrated in the narrowest angular range. However the product of the width and height of a mesa is not the same for all the heaters at a constant distance; it is largest for the narrowest heater. This product for the three heaters, at a given distance, increases with heater power density, and is approximately a universal function of heater power density rather than heater power.

A phenomenological model is proposed which explains the inverse relationship between sheet width and the heater width. The central feature of the model is that there is a critical energy density in the phonon shell which defines the edge of the mesa. This energy density is the critical energy density $\mathcal{E}_h$ for strong 3pp scattering which leads to an interacting l-phonon system, in anisotropic equilibrium, that just ceases to create h-phonons.

To obtain an expression for the energy density in the shell we make the approximation that the low energy phonons, in the angular regions where the l-phonons are noninteracting or weakly interacting, travel approximately in ballistic directions. This is justified by the fact that the three phonon interactions only involve small angles, especially for low energy phonons with energy well below 10 K. The energy density in the shell is then calculated assuming noninteracting ballistic propagation and is given in Eq. (5). The energy density is a strong function of angle because of the nonzero width of the heater, which means that phonons emitted from different points of the heater have different distances traveling to a point on the shell. The shell width is approximately the difference in distance traveled from the two edges of the heater, and is given by Eq. (3) and is illustrated in Fig. 12.

The edge of the mesa top is defined by the angle at which the energy density is equal to the critical energy density. However the critical energy density $\mathcal{E}_h$ is approximately proportional to the heater power. This can be seen in Fig. 11 by recognizing that the detected signal from the mesa top is proportional to the energy density in the shell. Hence the heater power nearly cancels out completely from Eq. (6) and we obtain the simple Eq. (9), where the weak heater power dependence is contained in the factor f. This explains why the size of the phonon sheet is only weakly dependent on heater power.

The model shows that the mesa width, which is $2\theta_A$, is inversely proportional to the heater width, as we found experimentally. It also shows that the mesa width is proportional to the heater pulse length, and data from Ref. 14 shows that this is so as long as the pulse length is short so that the h-phonons can escape the l-phonon pulse. The simple model has several approximations but nevertheless gives a reasonable description of all the measurements.

We thank I. N. Adamenko for useful discussions, R.V. Vovk for making the heaters and bolometers, and C. D. H. Williams for use of his program for some data analysis.

[1] A. F. G. Wyatt, M. A. H. Tucker, I. N. Adamenko, K. E. Nemchenko, and A. V. Zhukov, Phys. Rev. B **62**, 9402 (2000).
[2] M. A. H. Tucker and A. F. G. Wyatt, J. Phys.: Condens. Matter **6**, 2813 (1994).
[3] S. Havlin and M. Luban, Phys. Lett. **42**, 133 (1972).
[4] M. A. H. Tucker, A. F. G. Wyatt, I. N. Adamenko, A. V. Zhukov, and K. E. Nemchenko, Low Temp. Phys. **25**, 488 (1999) [Fiz. Nizk. Temp. **25**, 657 (1999)].
[5] I. N. Adamenko, K. E. Nemchenko, V. A. Slipko, Yu. A. Kitsenko, and A. F. G. Wyatt, Low Temp. Phys. **31**, 459 (2005) [Fiz. Nizk. Temp. **31**, 607 (2005)].
[6] M. A. H. Tucker and A. F. G. Wyatt, J. Phys.: Condens. Matter **4**, 7745 (1992).
[7] I. N. Adamenko, K. E. Nemchenko, and A. F. G. Wyatt, J. Low Temp. Phys. **125**, 1 (2001).
[8] I. N. Adamenko, K. E. Nemchenko, and A. F. G. Wyatt, J. Low Temp. Phys. **126**, 1471 (2002).
[9] H. J. Maris and W. E. Massey, Phys. Rev. Lett. **25**, 220 (1970).
[10] W. G. Stirling, in *75th Jubilee Conference on Liquid Helium-4*, edited by J. G. M. Armitage (World Scientific, Singapore, 1983), p. 109; private communication.
[11] M. A. H. Tucker and A. F. G. Wyatt, J. Phys.: Condens. Matter **6**, 2825 (1994).
[12] I. N. Adamenko, Y. A. Kitsenko, K. E. Nemchenko, V. A. Slipko, and A. F. G. Wyatt, Phys. Rev. B **73**, 134505 (2006).
[13] I. N. Adamenko, K. E. Nemchenko, A. V. Zhukov, M. A. H. Tucker, and A. F. G. Wyatt, Phys. Rev. Lett. **82**, 1482 (1999).
[14] R. V. Vovk, C. D. H. Williams, and A. F. G. Wyatt, Phys. Rev. B **68**, 134508 (2003).
[15] I. N. Adamenko, K. E. Nemchenko, V. A. Slipko, and A. F. G. Wyatt, J. Phys.: Condens. Matter **17**, 2859 (2005).
[16] I. N. Adamenko, K. E. Nemchenko, V. A. Slipko, and A. F. G. Wyatt, Phys. Rev. B **68**, 134507 (2003).
[17] I. N. Adamenko, K. E. Nemchenko, V. A. Slipko, and A. F. G. Wyatt, J. Low Temp. Phys. **138**, 67 (2005).
[18] D. H. S. Smith and A. F. G. Wyatt, Phys. Rev. B **76**, 224519 (2007).
[19] R. A. Sherlock and A. F. G. Wyatt, J. Phys. E **16**, 673 (1983).
[20] R. A. Sherlock, J. Phys. E **17**, 386 (1984).
[21] C. D. H. Williams, Meas. Sci. Technol. **1**, 322 (1990).
[22] D. H. S. Smith, R. V. Vovk, C. D. H. Williams, and A. F. G. Wyatt, New J. Phys. **8**, 128 (2006).
[23] P. C. Hendry and P. V. E. McClintock, Cryogenics **27**, 131 (1987).
[24] D. H. S. Smith, R. V. Vovk, C. D. H. Williams, and A. F. G. Wyatt, Phys. Rev. B **72**, 054506 (2005).
[25] R. V. Vovk, C. D. H. Williams, and A. F. G. Wyatt, Phys. Rev. B **69**, 144524 (2004).
[26] M. A. H. Tucker and A. F. G. Wyatt, J. Low Temp. Phys. **113**, 621 (1998).
[27] T. W. Bradshaw and A. F. G. Wyatt, J. Phys. C **16**, 651 (1983).